


Suppression and frequency control of repetitive spiking in the FitzHugh-Nagumo model

Hidetsugu Sakaguchi and Keito Yamasaki

Interdisciplinary Graduate School of Engineering Sciences, Kyushu University, Kasuga, Fukuoka 816-8580, Japan

 (Received 17 March 2023; accepted 7 July 2023; published 27 July 2023)

The FitzHugh-Nagumo equation is a simple model equation that exhibits spiking. The output signal of a neuron is represented in the spiking frequency or firing rate. We consider a few control methods for spiking from the viewpoint of nonlinear dynamics. The repetitive spiking can be suppressed in the FitzHugh-Nagumo model by the periodic sinusoidal force with high frequency. We study the transition to the suppressed state numerically and perform a linear stability analysis to understand the suppression of the spiking. Next, we study coupled FitzHugh-Nagumo equations. We find that the periodic forcing makes the system chaotic, and the desynchronization induced by chaos weakens the total output of spiking in a certain parameter range. Finally, we propose a method of feedback control for the spiking frequency. We can get the desired spiking and bursting frequency using this feedback control. The feedback control method is analyzed using a mapping for the input.

DOI: [10.1103/PhysRevE.108.014207](https://doi.org/10.1103/PhysRevE.108.014207)

I. INTRODUCTION

Neural systems exhibit various nonlinear dynamics. The Hodgkin-Huxley equation is a typical nonlinear equation that expresses the spiking of a giant axon of a squid [1]. A neuron is in a stationary state if there is no external input; however, it is excited and emits a spiking signal if the input to the neuron is beyond a threshold. The FitzHugh-Nagumo equation is a simple model equation that exhibits a similar spiking phenomenon [2,3]. Many authors have studied the Hodgkin-Huxley equation and the FitzHugh-Nagumo model from a viewpoint of nonlinear dynamics. For example, Holden studied the entrainment phenomena in the Hodgkin-Huxley equation under a periodic external force [4]. Rajasekar and Lakshmanan studied the period-doubling bifurcations and chaos in the FitzHugh-Nagumo model under the periodic forcing [5].

In general, the control methods of nonlinear systems have been studied by many authors [6,7]. The control of synchrony in coupled limit-cycle oscillators has also been studied by several authors [8,9]. The control of neural systems by external forces is important for the therapy of neurotic diseases. Deep brain stimulation (DBS) is used as a therapy for Parkinson's disease and essential tremors. In DBS for Parkinson's disease, high-frequency electrical stimulation is given to the subthalamic nucleus (STN) in the brain. Abnormal neuronal activity can be suppressed by DBS, although the mechanism is not completely understood [10]. Pyragas, Novicenko, and Tass studied the suppression of spontaneous oscillation of a single neuron by high-frequency stimulation using several model equations including the Hodgkin-Huxley equation and FitzHugh-Nagumo model [11].

We consider a few control methods for the spiking in the FitzHugh-Nagumo model from the viewpoint of nonlinear dynamics. In Sec. II, we study the suppression of the spiking by high-frequency stimulation for the FitzHugh-Nagumo equation again. We study the transition to the suppressed state more in detail. In Sec. III, we study the suppression and

desynchronization in coupled FitzHugh-Nagumo equations, since the neural system can be described as a coupled system of many neurons. In Sec. IV, we propose a simple control method for the spiking frequency. We can get the spiking and bursting frequencies we want with the feedback control. An approximate map for the effective input is derived and the analysis is compared with the direct numerical simulation. In Sec V, we summarize the results.

II. SUPPRESSION OF REPETITIVE SPIKING IN THE FITZHUGH-NAGUMO MODEL BY PERIODIC FORCES

The FitzHugh-Nagumo model is a simple model equation of excitable and oscillatory systems. In this paper, we study a modified model equation of the form

$$\begin{aligned}\frac{du}{dt} &= u(u+a)(1-u) - v, \\ \frac{dv}{dt} &= \epsilon(u - bv).\end{aligned}\quad (1)$$

This equation has third-order nonlinearity. The nullclines are expressed as $v = u(u+a)(1-u)$ and $v = u/b$. The origin $u = v = 0$ is always a stationary solution. It can be predicted from the nullclines that the system becomes excitatory for $a < 0$ and oscillatory for $a > 0$ if ϵ is sufficiently small. This is a useful point of this model in contrast to the standard FitzHugh-Nagumo model:

$$\begin{aligned}\frac{dx}{dt'} &= x - \frac{x^3}{3} - y, \\ \frac{dy}{dt'} &= \epsilon'(x - c - dy).\end{aligned}\quad (2)$$

The standard FitzHugh-Nagumo model (2) can be derived from Eq. (1) by the change of variables: $x = 3/\sqrt{1+a+a^2}\{u - (1-a)/3\}$, $y = 9/(1+a+a^2)^{3/2}\{v - (1-a)(1+2a)(2+a)/27\}$, and $t' = (1+a+a^2)/3t$.

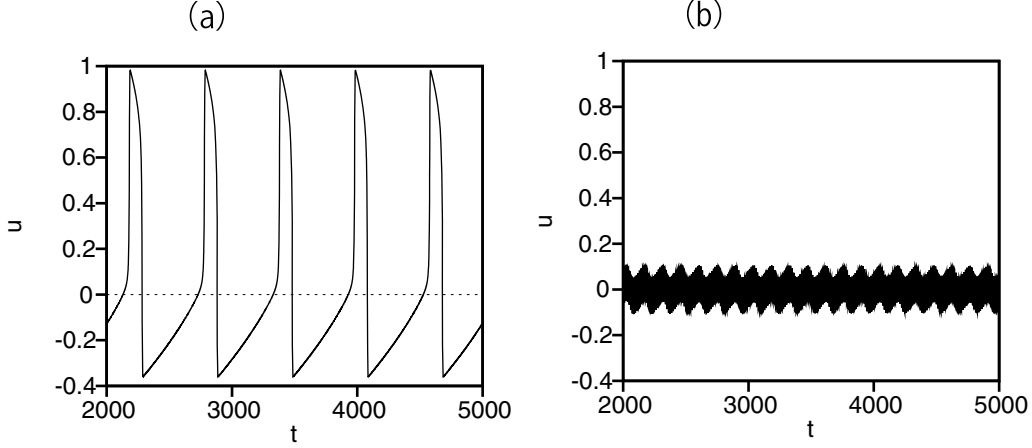


FIG. 1. Time evolutions of $u(t)$ at (a) $F = 0$ and (b) $F = 0.04$ at $a = 0.01$, $\epsilon = 0.002$, and $\omega = 0.5$.

In this section, we consider Eq. (1) with $b = 0$ for the sake of simplicity. The linear perturbations δu and δv around $u = v = 0$ satisfy

$$\begin{aligned} \frac{d\delta u}{dt} &= a\delta u - \delta v, \\ \frac{d\delta v}{dt} &= \epsilon\delta u. \end{aligned} \quad (3)$$

The eigenvalue λ satisfies

$$\lambda^2 - a\lambda + \epsilon = 0$$

and is expressed explicitly as

$$\lambda = \frac{a \pm \sqrt{a^2 - 4\epsilon}}{2}.$$

When $a > 0$, the stationary solution becomes unstable, which leads to periodic excitation of the large amplitude of $O(1)$.

When a periodic force is applied to the equation of u , Eq. (1) becomes

$$\begin{aligned} \frac{du}{dt} &= u(u+a)(1-u) - v + F \sin \omega t, \\ \frac{dv}{dt} &= \epsilon u. \end{aligned} \quad (4)$$

When high-frequency stimulation is applied, there is a possibility that repetitive spiking is suppressed. The zeroth approximation of the solution to Eq. (4) is expressed as

$$u = u_c \cos \omega t + u_s \sin \omega t, \quad v = v_0$$

where u_c and u_s satisfy

$$\begin{aligned} -\omega u_c \sin \omega t + \omega u_s \cos \omega t \\ \simeq F \sin \omega t + a(u_c \cos \omega t + u_s \sin \omega t). \end{aligned}$$

Therefore, u_c , u_s , and v_0 satisfy

$$u_c \simeq -\frac{F\omega}{\omega^2 + a^2}, \quad u_s = -\frac{Fa}{\omega^2 + a^2}, \quad v_0 = (1-a)\frac{F^2}{2(\omega^2 + a^2)}.$$

When a is sufficiently small, $u_c \simeq -F/\omega$, $u_s \simeq 0$, and $v_0 \simeq (1-a)F^2/(2\omega^2)$.

We assume a solution of the form

$$u = u_c \cos \omega t + \delta u, \quad v = v_0 + \delta v. \quad (5)$$

Using the approximation $u^3 \simeq u_c^3 \cos^3 \omega t + 3u_c^2 \cos^2 \omega t \delta u$ and $u^2 \simeq u_c^2 \cos^2 \omega t + 2u_c \cos \omega t \delta u$, linearized equations for δu and δv are obtained as

$$\begin{aligned} \frac{d\delta u}{dt} &= \{a - 3F^2/\omega^2 \cos^2 \omega t + 2(1-a)u_c \cos \omega t\} \delta u - \delta v, \\ \frac{d\delta v}{dt} &= \epsilon \delta u. \end{aligned} \quad (6)$$

If $\cos^2 \omega t \simeq 1/2$ and $\cos \omega t \simeq 0$ are assumed by the temporal average, Eq. (6) becomes

$$\begin{aligned} \frac{d\delta u}{dt} &= \{a - 3F^2/(2\omega^2)\} \delta u - \delta v, \\ \frac{d\delta v}{dt} &= \epsilon \delta u. \end{aligned} \quad (7)$$

If $\delta u = \delta u_0 e^{\lambda t}$ and $\delta v = \delta v_0 e^{\lambda t}$ are substituted into Eq. (7), the linear growth rate λ is evaluated as

$$\lambda = \frac{[a - (3/2)F^2/\omega^2] \pm \sqrt{[a - (3/2)F^2/\omega^2]^2 - 4\epsilon}}{2}.$$

If $a < (3/2)F^2/\omega^2$, then $\text{Re}\lambda < 0$ and δu and δv decay to zero, that is, the periodic solution $u = u_c \cos \omega t$ of small amplitude is stabilized. This implies that the repetitive spiking of large amplitude is suppressed. This mechanism is almost the same as the one proposed by Pyragas *et al.* [11].

We have performed a numerical simulation of Eq. (4) with the Runge-Kutta method. Figures 1(a) and 1(b) show time evolutions of $u(t)$ at (a) $F = 0$ and (b) $F = 0.04$ for $a = 0.01$, $\epsilon = 0.002$, and $\omega = 0.5$. The initial condition is $u = 0.1$ and $v = 0.1$. At $F = 0$, repetitive spiking is observed. The period is $T \simeq 600$. The oscillation of large amplitude is suppressed at $F = 0.04$ for the frequency $\omega = 0.5$ which is around 48 times larger than $2\pi/T$. Figure 2(a) shows the right and left boundaries in the parameter space of (ω, F) . The repetitive spiking is suppressed in a parameter region between the two boundaries. The left boundary is a new finding in our numerical simulation. There is a minimum value $F_c \simeq 0.0135$ for the amplitude F around $\omega = 0.176$ to suppress the repetitive

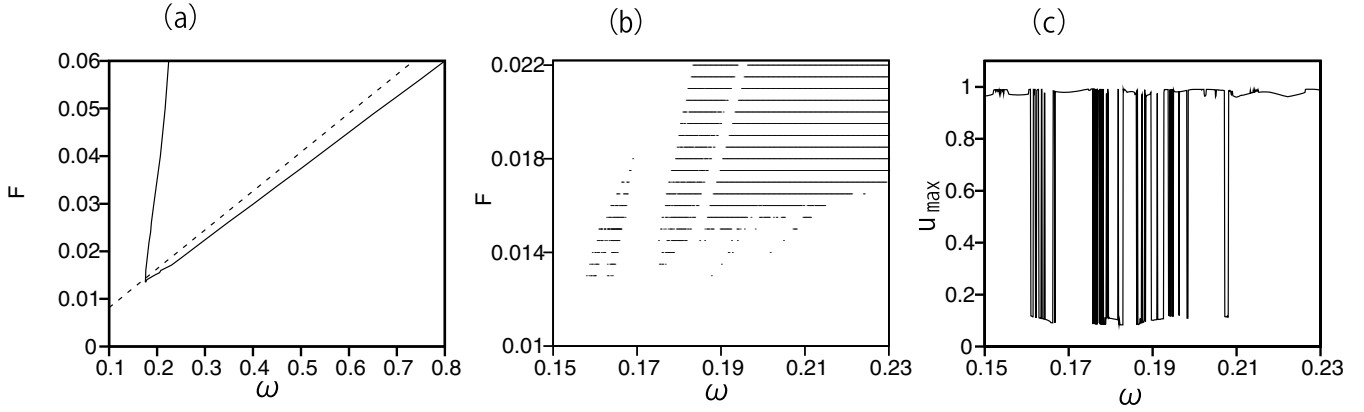


FIG. 2. (a) Boundary lines in the parameter space of (ω, F) above which the repetitive pulsation is suppressed. The dashed line is $F = \sqrt{2a/3}\omega$. (b) Parameter values of ω and F where the repetitive pulsation is suppressed. Magnification of the phase diagram in (a) around $\omega = 0.2$ and $F = 0.016$. (c) Maximum value of u as a function of ω at $F = 0.015$.

spiking since the parameter region of the suppressed state is bounded by the two boundary lines. The dashed line denotes a theoretical approximation $F_c = \sqrt{2a/3}\omega$ by the linear equation Eq. (7). The theoretical line is a good approximation of the right boundary. The phase boundary is complicated near the critical parameter $\omega = 0.176$ and $F = 0.0135$ where the two boundary lines meet as shown in Fig. 2(b). Figure 2(c) is the maximum value of u as a function of ω at $F = 0.015$. The maximum value takes a value near 1 when the repetitive spiking occurs, and a value near 0.1 when the suppression occurs. This figure shows that the occurrence of suppression depends on ω sensitively at $F = 0.015$.

Figure 3(a) shows the maximum value of u for $0.2069 < \omega < 0.207$ at $F = 0.04$ near the left boundary. The transition to the suppressed state occurs at $\omega = 0.206988$. Figure 3(b) shows the time evolution of u at $\omega = 0.2069$, where the spiking appears intermittently. We have calculated the Lyapunov exponent near this parameter value. The Lyapunov exponent is positive, which implies that the system is chaotic.

The right boundary of the phase diagram was understood by the linear equation Eq. (7) but the left boundary cannot be reproduced by Eq. (7). To understand the left boundary, we consider the linearized equation Eq. (6) again. Here,

$\cos^2 \omega t \simeq 1/2$ is assumed but we retain the periodic modulation term $2(1-a)u_c \cos(\omega t)\delta u$. Therefore, δu and δv obey

$$\begin{aligned} \frac{d\delta u}{dt} &= \{a - 3F^2/(2\omega^2) - 2(1-a)(F/\omega) \cos \omega t\} \delta u - \delta v, \\ \frac{d\delta v}{dt} &= \epsilon \delta u. \end{aligned} \quad (8)$$

We have studied the stability by direct numerical simulations of Eq. (8) and found that there are two types of boundaries. Figure 4(a) shows the two boundaries obtained by the numerical simulations of Eq. (8). The right boundary line is well approximated by $F = \sqrt{2a/3}\omega$ even in this model. We have further simplified the linearized equation with time-periodic modulation by assuming that $-\cos \omega t = 1/\sqrt{2}$ for $\pi/2 < \omega t < 3\pi/2$ and $-\cos \omega t = -1/\sqrt{2}$ for $3\pi/2, \omega t < 5\pi/2$. Here, $1/\sqrt{2}$ is the root mean square value of $\cos \omega t$. The coupled piecewise linear equations are explicitly written as

$$\begin{aligned} \frac{d\delta u}{dt} &= \{a - 3F^2/(2\omega^2) + 2(1-a)F/(\sqrt{2}\omega)\} \delta u - \delta v, \\ \frac{d\delta v}{dt} &= \epsilon \delta u \end{aligned} \quad (9)$$

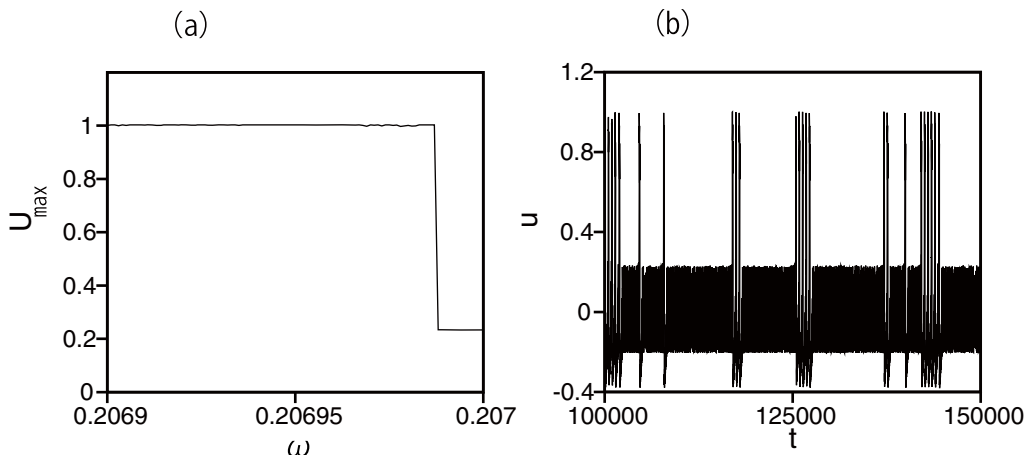


FIG. 3. (a) Maximum value of u for $0.2069 < \omega < 0.207$ at $F = 0.04$ near the left boundary. (b) Time evolution of u at $\omega = 0.2069$ and $F = 0.04$.

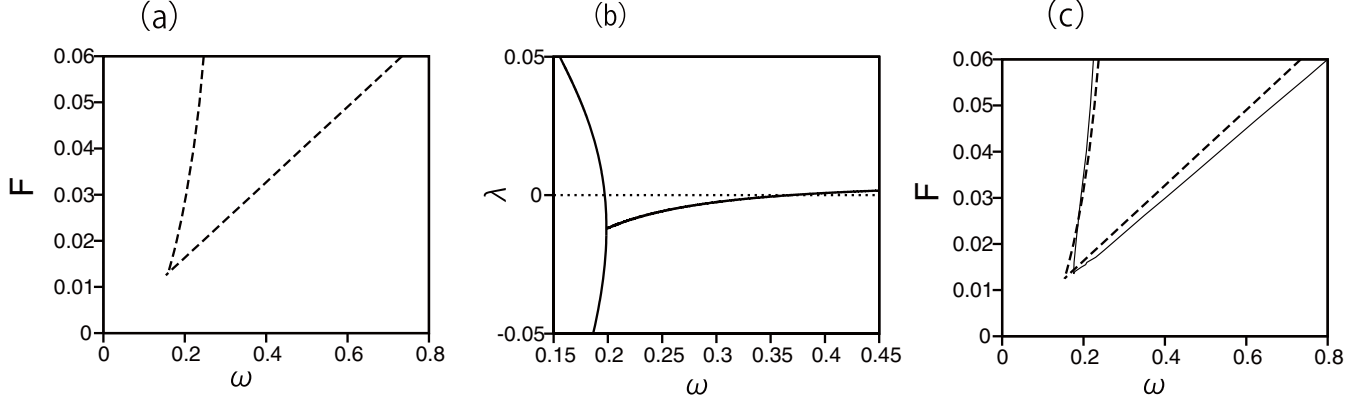


FIG. 4. (a) Two boundary lines evaluated by numerical simulations of Eq. (8). (b) $\lambda = \log |\mu|/(2\pi/\omega)$ for $0.15 \leq \omega \leq 0.45$ at $F = 0.03$. (c) Two boundary lines (dashed lines) evaluated by the eigenvalues of the linear transformation Eq. (13) and two boundary lines as shown in Fig. 2(a). The parameter values a and ϵ are $a = 0.01$ and $\epsilon = 0.002$.

for $\pi/2 < \omega t < 3\pi/2$, and

$$\begin{aligned} \frac{d\delta u}{dt} &= \{a - 3F^2/(2\omega^2) - 2(1-a)F/(\sqrt{2}\omega)\}\delta u - \delta v, \\ \frac{d\delta v}{dt} &= \epsilon\delta u \end{aligned} \quad (10)$$

for $3\pi/2 < \omega t < 5\pi/2$. The linear equation can be solved by the eigenvalues and eigenvectors of the coefficient matrix of the coupled linear differential equations. The eigenvalues of Eq. (9) are

$$\lambda_1 = \frac{a - 3F^2/(2\omega^2) + 2(1-a)F/(\sqrt{2}\omega) + \sqrt{\{a - 3F^2/(2\omega^2) + 2(1-a)F/(\sqrt{2}\omega)\}^2 - 4\epsilon}}{2}$$

and $\lambda_2 = \epsilon/\lambda_1$. The right and left eigenvectors for the eigenvalue λ_1 are respectively ${}^t(1, \epsilon/\lambda_1)$ and $(1/(1 - \epsilon/\lambda_1^2), -1/(\lambda_1 - \epsilon/\lambda_1))$. The right and left eigenvectors for the eigenvalue λ_2 are respectively ${}^t(1, \lambda_1)$ and $(\epsilon/(\epsilon - \lambda_1^2), -\lambda_1/(\epsilon - \lambda_1^2))$. Using the eigenvalues and eigenvectors, a linear transformation of $(\delta u(t), \delta v(t))$ from $t_1 = \pi/(2\omega)$ to $t_2 = 3\pi/(2\omega)$ is written as

$$\begin{pmatrix} \delta u(t_2) \\ \delta v(t_2) \end{pmatrix} = A \begin{pmatrix} \delta u(t_1) \\ \delta v(t_1) \end{pmatrix}, \quad (11)$$

where the matrix A is

$$A = \frac{e^{\lambda_1\pi/\omega}}{1 - \epsilon/\lambda_1^2} \begin{pmatrix} 1 & -1/\lambda_1 \\ \epsilon/\lambda_1 & -\epsilon/\lambda_1^2 \end{pmatrix} + \frac{e^{\epsilon\pi/(\lambda_1\omega)}}{1 - \lambda_1^2/\epsilon} \begin{pmatrix} 1 & -\lambda_1/\epsilon \\ \lambda_1 & -\lambda_1^2/\epsilon \end{pmatrix}.$$

Similarly, the eigenvalues of Eq. (10) are

$$\lambda_3 = \frac{a - 3F^2/(2\omega^2) - 2(1-a)F/(\sqrt{2}\omega) - \sqrt{\{a - 3F^2/(2\omega^2) - 2(1-a)F/(\sqrt{2}\omega)\}^2 - 4\epsilon}}{2}$$

and $\lambda_4 = \epsilon/\lambda_3$. The right and left eigenvectors for the eigenvalue λ_3 are respectively ${}^t(1, \epsilon/\lambda_3)$ and $(1/(1 - \epsilon/\lambda_3^2), -1/(\lambda_3 - \epsilon/\lambda_3))$. The right and left eigenvectors for the eigenvalue λ_4 are respectively ${}^t(1, \lambda_3)$ and $(\epsilon/(\epsilon - \lambda_3^2), -\lambda_3/(\epsilon - \lambda_3^2))$. Using the eigenvalues and eigenvectors, a linear transformation of $(\delta u(t), \delta v(t))$ from $t_2 = 3\pi/(2\omega)$ to $t_3 = 5\pi/(2\omega)$ is written as

$$\begin{pmatrix} \delta u(t_3) \\ \delta v(t_3) \end{pmatrix} = B \begin{pmatrix} \delta u(t_2) \\ \delta v(t_2) \end{pmatrix}, \quad (12)$$

where the matrix B is

$$B = \frac{e^{\lambda_3\pi/\omega}}{1 - \epsilon/\lambda_3^2} \begin{pmatrix} 1 & -1/\lambda_3 \\ \epsilon/\lambda_3 & -\epsilon/\lambda_3^2 \end{pmatrix} + \frac{e^{\epsilon\pi/(\lambda_3\omega)}}{1 - \lambda_3^2/\epsilon} \begin{pmatrix} 1 & -\lambda_3/\epsilon \\ \lambda_3 & -\lambda_3^2/\epsilon \end{pmatrix}.$$

The linear transformation from $t = t_1$ to t_3 is expressed as

$$\begin{pmatrix} \delta u(t_3) \\ \delta v(t_3) \end{pmatrix} = BA \begin{pmatrix} \delta u(t_1) \\ \delta v(t_1) \end{pmatrix}. \quad (13)$$

If the absolute value of the eigenvalues μ of the matrix BA is smaller than 1, δu and δv decay to zero, and the repetitive spiking is suppressed. Figure 4(b) shows $\lambda = \log |\mu|/(2\pi/\omega)$ for $0.15 \leq \omega \leq 0.45$ at $F = 0.03$. For $\omega > 0.1987$, the eigenvalue μ is a complex number and λ increases slowly and becomes positive at $\omega = 0.3675$. For $\omega < 0.1987$, two real eigenvalues μ_+ and μ_- appear for the matrix BA , and $\lambda_+ = \log |\mu_+|/(2\pi/\omega)$ decreases rapidly with ω near $\omega = 0.1987$ and becomes positive for $\omega < 0.1971$. $\omega = 0.1971$ is the left boundary of the stability of the linear equations expressed

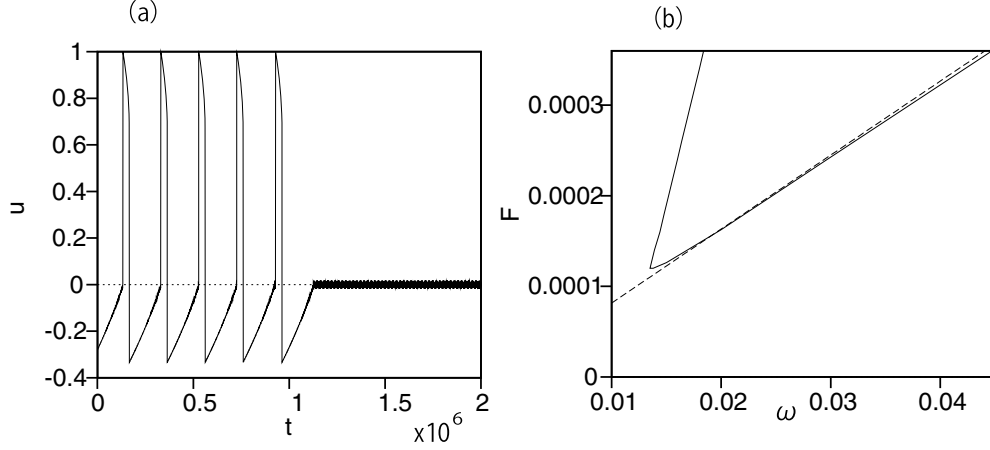


FIG. 5. (a) Time evolutions of $u(t)$ at $F = 0.003$ and $\omega = 0.0172$ for $a = 0.0001$ and $\epsilon = 5 \times 10^{-6}$. (b) Boundary lines in the parameter space of (ω, F) above which the repetitive pulsation is suppressed for $a = 0.0001$ and $\epsilon = 5 \times 10^{-6}$. The dashed line is $F = \sqrt{2a/3}\omega$.

by Eqs. (9) and (10). Figure 4(c) shows the right and left boundary lines of $\lambda_+ = 0$. At the left boundary, the real eigenvalue μ_+ becomes -1 . At the right boundary, μ is a complex number and the absolute value becomes 1. The right boundary is almost equal to $F = \sqrt{2a/3}\omega$.

When a and ϵ are smaller, the critical value of F becomes even smaller. We have performed numerical simulation at $a = 0.0001$ and $\epsilon = 5 \times 10^{-6}$. Figure 5(a) shows a time evolution of u at $F = 0.003$ and $\omega = 0.0172$. The spiking is suppressed after the fifth spiking, and the suppressed state with high-frequency modulation appears. Figure 5(b) shows the parameter range of the suppression of spiking. The dashed line is $F_c = \sqrt{2a/3}\omega$. The approximation is very good for this parameter set. The minimum value of F is 0.0012, which is much smaller than the critical value shown in Fig. 2(a).

The suppression of neuronal spiking by high-frequency forcing is observed in other systems. Pyragas *et al.* studied the suppression in the Hodgkin-Huxley equation and STN model [11]. However, the lower limit of the frequency was not studied in detail. We have studied a parameter range of the suppression in the Hodgkin-Huxley equation. The model equation is expressed as

$$\begin{aligned}
 C_m \frac{dV}{dt} &= g_{Na} m^3 h (E_{Na} - V) + g_K n^4 (E_K - V) + g_L (E_L - V) \\
 &\quad + I_0 + I_1 \cos 2\pi f t, \\
 \frac{dm}{dt} &= \alpha_m - (\alpha_m + \beta_m) m, \\
 \frac{dh}{dt} &= \alpha_h - (\alpha_h + \beta_h) h, \\
 \frac{dn}{dt} &= \alpha_n - (\alpha_n + \beta_n) n,
 \end{aligned} \tag{14}$$

where $E_{Na} = 115$, $E_K = -12$, $E_L = -10.6$, $g_{Na} = 120$, $g_K = 36$, and $g_L = 0.3$. $\alpha_m \sim \alpha_n$ are functions of V as

$$\begin{aligned}
 \alpha_m &= \frac{(V - 25)/10}{1 - \exp\{-(V - 25)/10\}}, \quad \beta_m = 4 \exp\{-V/18\}, \\
 \alpha_h &= 0.07 \exp\{-V/20\}, \quad \beta_h = \frac{1}{1 + \exp\{-(V - 30)/10\}}, \\
 \alpha_n &= \frac{0.01(V - 10)}{1 - \exp\{-(V - 10)/10\}}, \quad \beta_n = 0.125 \exp\{-V/80\}.
 \end{aligned} \tag{15}$$

The average current I_0 is set to 20. Figures 6(a) and 6(b) show the time evolutions of V at (a) $I_1 = 350$ and (b) $I_1 = 400$ and $f = 5$. The initial values of V , m , h , and n are zero. The suppression of spiking occurs at $I_1 = 400$. Figure 6(c) shows a critical line in the (f, I_1) space above which the suppression is observed. The critical line decreases rapidly near $f = 1.46$. It implies that the suppression is hard for the lower frequency $f < 1.46$. There seems to be only one critical line, which is different from the case of the FitzHugh-Nagumo model. There is a minimum amplitude $I_1 \simeq 202.8$ for the suppression at $f = 1.9$. The existence of the minimum amplitude is the same as the case of the FitzHugh-Nagumo model.

III. DESYNCHRONIZATION OF SPIKING IN COUPLED FITZHUGH-NAGUMO EQUATIONS BY PERIODIC FORCES

Neurons interact with each other in a complicated manner in real neural networks in brains. As one of the simplest models, we study globally coupled FitzHugh-Nagumo equations:

$$\begin{aligned}
 \frac{du_i}{dt} &= u_i(u_i + a)(1 - u_i) - v_i + F \sin \omega t + \frac{K}{N} \sum_{j=1}^N (u_j - u_i), \\
 \frac{dv_i}{dt} &= \epsilon u_i, \quad \text{for } i = 1, 2, \dots, N
 \end{aligned} \tag{16}$$

where K is the coupling constant and N is the total number of neurons. The parameters a and ϵ are fixed to be $a = 0.01$ and $\epsilon = 0.002$. The total number N is assumed to be 1000.

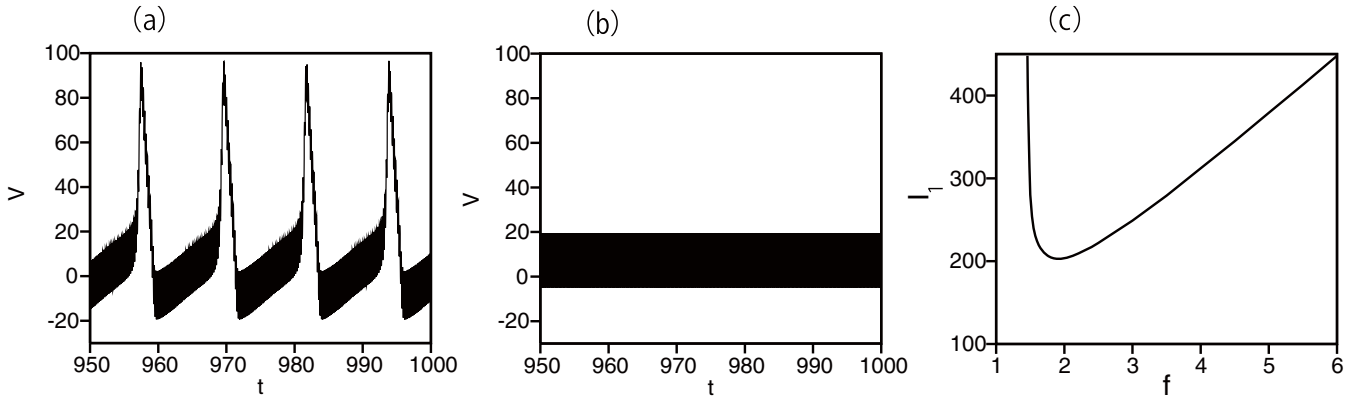


FIG. 6. Time evolutions of V in the forced Hodgkin-Huxley equation Eq. (14) at (a) $I_1 = 350$ and (b) $I_1 = 400$ for $f = 5$. (c) Critical line in the (f, I_1) space above which the suppression is observed.

As shown in the previous section, the suppression of spiking does not occur for small values of $\omega < 0.17$ in a single FitzHugh-Nagumo equation. However, a weak chaos can occur in the single FitzHugh-Nagumo equation. Figure 7(a) shows a time evolution of u at $\omega = 0.1$ and $F = 0.0074$ for the FitzHugh-Nagumo equation Eq. (4). Almost periodic spiking is observed; however, the temporal modulation below the threshold is not periodic but chaotic. Figure 7(b) shows the Lyapunov exponent as a function of F at $\omega = 0.1$ for Eq. (4). Weak chaos appears for $0.0071 \leq \omega \leq 0.0078$.

In coupled oscillator systems, the limit-cycle oscillators tend to be synchronized even for very small $K > 0$. However, the synchronization does not occur for chaotic oscillators if K is smaller than a critical value K_c [12,13]. In a globally coupled system like Eq. (16), the chaos induces desynchronization for small K and the average value $\bar{u} = \sum_{j=1}^N u_j/n$ does not show spiking even if each oscillator exhibits spiking, because the timing of the spiking is randomly distributed. There is a transition from the desynchronized state to the synchronized state as K is increased [14]. Figure 8(a) shows the time evolutions of \bar{u} (solid line) and u_i (dashed line, $i = 750$) in Eq. (14) at $K = 0.0001$, $\omega = 0.1$, and $F = 0.0074$. The spiking is observed for u_i ; however, small-amplitude fluctuations are observed in the time evolution of \bar{u} . Figure 8(b) shows (u_i, v_i) ($i = 1, 2, \dots, 1000$) at $t = 50\,000$ in the phase

space of u and v . The distribution of (u_i, v_i) implies the desynchronization. The desynchronization makes the total activity in the globally coupled system depressed. Figure 8(c) shows the peak value of $\bar{u}(t)$ as a function of F at $\omega = 0.1$ and $K = 0.0001$. The average value $\bar{u}(t)$ decreases from around 1 to around 0.1 for $0.0071 \leq \omega \leq 0.0078$. The parameter range is the same as the one where the weak chaos appears in the single FitzHugh-Nagumo equation. The desynchronization is observed for sufficiently small K . We have studied the transition from the desynchronized state to a synchronized state as K is increased at $F = 0.074$ and $\omega = 0.1$ for $N = 1000$. The single FitzHugh-Nagumo model exhibits chaos by the periodic forcing at $F = 0.074$ and $\omega = 0.1$. We have calculated the root mean square $\Delta u = \langle (\bar{u}(t) - \langle \bar{u} \rangle)^2 \rangle^{1/2}$ of $u(t)$. Here, $\langle z \rangle$ denotes the temporal average of $z(t)$. The root mean square Δu increases with K and a completely synchronized state is attained at $K = 0.012$. At intermediate values of K , various partially synchronized states appear. Figure 8(d) shows the time evolutions of \bar{u} (solid line) and u_i (dashed line, $i = 750$) at $K = 0.005$, $\omega = 0.1$, and $F = 0.0074$. At the parameter values, a three-cluster state is observed. That is, the 1000 neural oscillators are split into three clusters of 99, 556, and 345 oscillators. In each cluster, oscillators are mutually synchronized. The time evolution of \bar{u} exhibits three peaks, because of the three synchronized clusters.

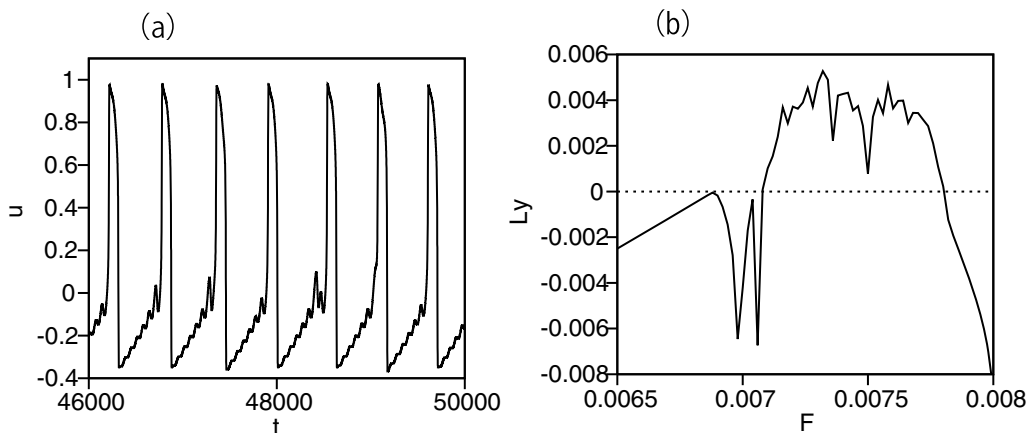


FIG. 7. (a) Time evolution of u at $F = 0.0074$ and $\omega = 0.1$ for Eq. (4). (b) Lyapunov exponent as a function of F at $\omega = 0.1$.

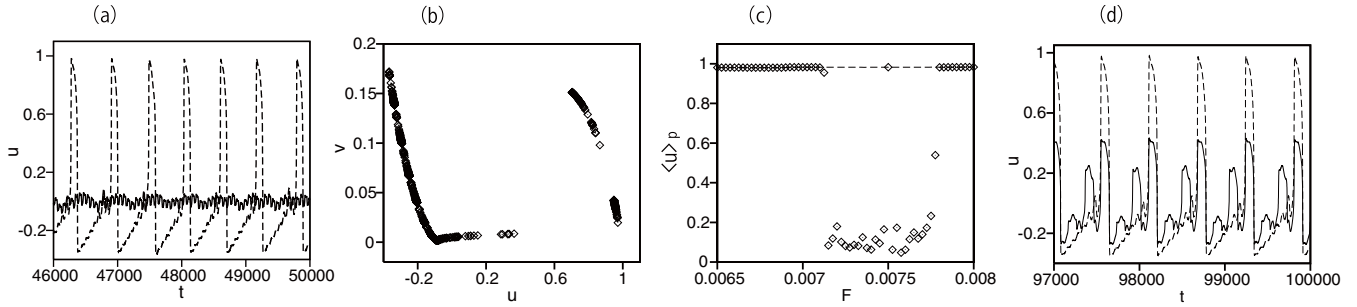


FIG. 8. (a) Time evolutions of \bar{u} (solid line) and u_i (dashed line, $i = 750$) in Eq. (16) at $K = 0.0001$, $\omega = 0.1$, and $F = 0.0074$. (b) Plot of (u_i, v_i) ($i = 1, 2, \dots, 1000$) at $t = 50\,000$ in the phase space of u and v . (c) Peak value of \bar{u} as a function of F at $\omega = 0.1$ and $K = 0.0001$. (d) Time evolutions of \bar{u} (solid line) and u_i (dashed line, $i = 750$) at $K = 0.005$, $\omega = 0.1$, and $F = 0.0074$.

The mean-field type coupling as in Eq. (16) is not realistic in actual neural networks. Gerster *et al.* studied the FitzHugh-Nagumo oscillators on complex networks [15]. Here, we show some numerical results of a random network where the coupling is randomly cut off with probability p from the globally coupled system. The model equation is expressed as

$$\begin{aligned} \frac{du_i}{dt} &= u_i(u_i + a)(1 - u_i) - v_i + F \sin \omega t \\ &+ K \sum_{j=1}^N A_{i,j}(u_j - u_i), \\ \frac{dv_i}{dt} &= \epsilon u_i, \end{aligned} \tag{17}$$

where $A_{i,j}$ takes zero with probability p and 1 with probability $1 - p$. We have performed numerical simulation at $F = 0.074$, $\omega = 0.1$, and $p = 0.7$ for $N = 200$. The single FitzHugh-Nagumo oscillator exhibits chaos. Figure 9(a) shows the root mean square Δu as a function of K . The root mean square increases with K from $K \simeq 0.000\,01$. Figure 9(b) shows the time evolutions of \bar{u} (solid line) and u_i (dashed line, $i = 50$) at $K = 0.000\,01$. A desynchronized state appears even in this random neural network. Figure 9(c) shows the time evolutions of \bar{u} (solid line) and u_i (dashed line, $i = 50$) at $K = 0.000\,05$. A partially synchronized state appears in this coupling strength.

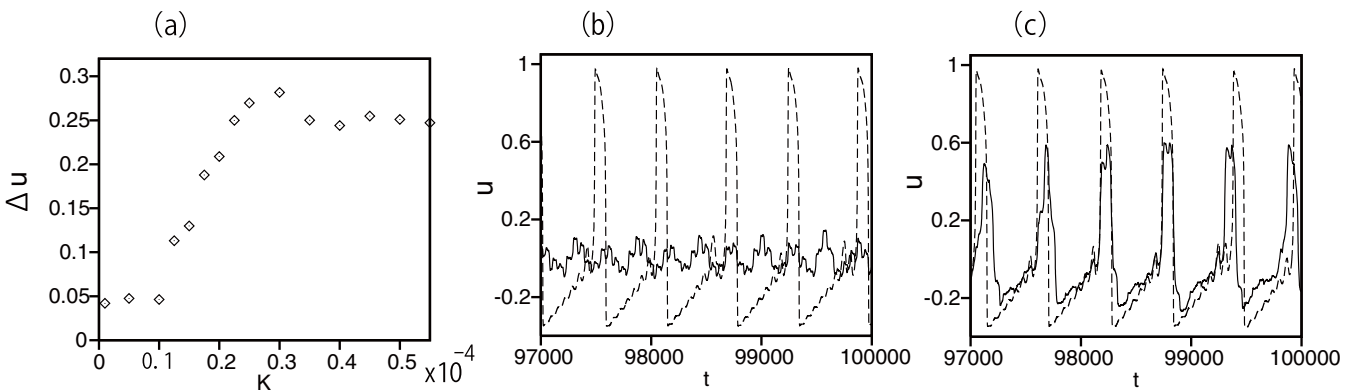


FIG. 9. (a) Root mean square Δu as a function of K in a random network of FitzHugh-Nagumo oscillators at $F = 0.074$, $\omega = 0.1$, and $p = 0.7$. (b) Time evolutions of \bar{u} (solid line) and u_i (dashed line, $i = 50$) at $K = 0.000\,01$. (c) Time evolutions of \bar{u} (solid line) and u_i (dashed line, $i = 50$) at $K = 0.000\,05$.

To summarize this section, the periodic forcing can generate weak chaos in some parameter ranges, which induces desynchronization in coupled systems. The spiking disappears in the average activity in the coupled system. The collective spiking by the synchronization induces a negative effect such as tremors. Desynchronization might be another mechanism for the success of DBS.

IV. FEEDBACK CONTROL OF SPIKING FREQUENCY IN THE FITZHUGH-NAGUMO MODEL

In this section, we consider the FitzHugh-Nagumo model of the form

$$\begin{aligned} \frac{du}{dt} &= u(u + a)(1 - u) - v + I, \\ \frac{dv}{dt} &= \epsilon(u - bv), \end{aligned} \tag{18}$$

where $a = 0.02$ and $\epsilon = 0.002$. Figure 10(a) shows the period T of the repetitive spiking as a function of the input I for $b = 0$ (dashed line) and $b = 1$ (solid line). The period does not depend on I at $b = 0$, because Eq. (18) is transformed to Eq. (1) by the change of variable: $v - I \rightarrow v$. However, the period T decreases with I and diverges near $I = -0.008\,718$ at $b = 1$. For $0 < b < 1$, a similar behavior to the case of $b = 1$ is observed, although the critical value of I for spiking increases with b . Figure 10(b) shows the trajectories in the

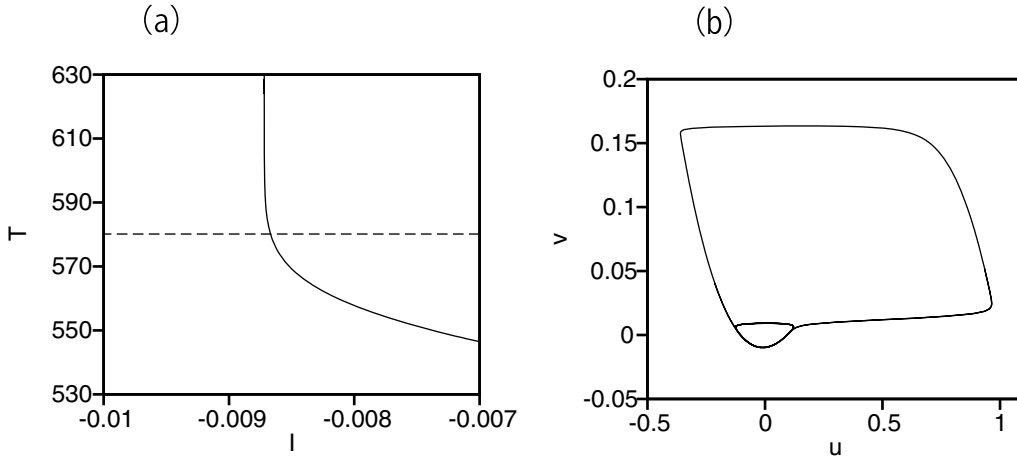


FIG. 10. (a) Period T of the repetitive spiking as a function of I for $b = 0$ (dashed line) and $b = 1$ (solid line). (b) Trajectories at $I = -0.00871807$ (large loop) and -0.00871806 [small loop around $(u, v) = (0, 0)$] for $b = 1$.

phase space (u, v) at $I = -0.00871806$ and -0.00871807 for $b = 1$. There is a transition from the limit-cycle oscillation of large amplitude at $I = -0.00871806$ to that of small amplitude at $I = -0.00871807$. Repetitive spiking is observed at $I = -0.00871806$ but the spiking does not occur at $I = -0.00871807$.

To control the spiking frequency, we consider a model equation where I changes with time:

$$\begin{aligned} \frac{du}{dt} &= u(u+a)(1-u) - v + I_n, \\ \frac{dv}{dt} &= \epsilon(u-v), \\ \frac{dI}{dt} &= \epsilon' \left(\frac{1}{T_p} - \delta(u-u_0)\theta(du/dt) \right) \end{aligned} \quad (19)$$

where $a = 0.02$, $\epsilon = 0.002$, $u_0 = 0.5$, $\epsilon' = 0.00005$, $\delta(x)$ is the delta function, and $\theta(x)$ is the Heaviside step function which takes 1 only for $x > 0$. $I(t)$ increases constantly with ϵ'/T_p owing to the first term of the third equation in Eq. (19). On the other hand, $I(t)$ decreases by ϵ' when u passes through $u = u_0$ under the condition of $du/dt > 0$. The input I_n for u takes a constant value $I(t_n)$ between $t_n \leq t < t_{n+1}$, where t_n is the time just before the passage through $u = u_0$. In other words, the input for u changes stepwise when u passes through $u = u_0$ under the condition of $du/dt > 0$.

If the spiking period T is larger than T_p in Eq. (19), I tends to increase on average and the spiking period decreases. On the other hand, if the spiking period T is smaller than T_p , I tends to decrease on average and the spiking period increases. Owing to the negative feedback effect, the spiking period T_p is finally obtained if the control succeeds. Figure 11(a) shows the time evolution of I at $T_p = 600$, $\epsilon' = 0.00005$, and $b = 1$. Figure 11(b) shows the time evolution of the spiking period in the same numerical simulation. Initially, I is set to be zero. I decreases with time and the period approaches the goal value $T_p = 600$. Figure 11(c) is the time evolution of u after the feedback control, which demonstrates that the periodic pulsation of $T = 600$ is reproduced.

Figure 12(a) shows the relationship between T_p and I after the feedback control at $b = 1$ for $\epsilon' = 0.00005$. $T = T_p$ is attained until $T_p = T_{pc} = 608.7$. However, a period-doubling bifurcation occurs, and the stable stationary solution cannot be obtained for $T_p > T_{pc}$. This is probably due to the steep slope of the $T(I)$ curve in Fig. 10(a). Figure 12(b) shows a relationship between T_p and I after the feedback control at $b = 1$ for $\epsilon' = 0.00001$. At $\epsilon' = 0.00001$, $T = T_p$ is attained until $T_p = T_{pc} = 615.96$. A similar period-doubling bifurcation occurs at the critical value. The feedback control succeeds for a wider parameter range for smaller ϵ' .

Figure 13(a) shows the relationship between I_n and I_{n+1} where I_n is the input for u and equal to $I(t_n)$ just before the m th passage time t_m of $u = u_0$ with $du/dt > 0$. The parameter values are $T_p = 609.93$ and $\epsilon' = 0.00005$, where a chaotic behavior is observed in Fig. 12(a). A parabolalike curve is observed. The chaotic behavior is caused by the parabolalike mapping, which is similar to the chaos in the logistic map. From the differential equation of $I(t)$ in Eq. (19), the mapping from I_n to I_{n+1} can be approximately constructed as

$$I_{n+1} = I_n + \epsilon' \frac{T(I_n)}{T_p} - \epsilon'. \quad (20)$$

This is because I decreases suddenly by ϵ' at $t = t_n$ and increases steadily with the rate ϵ'/T_p during a period from the n th to $(n+1)$ th passing of $u = u_0$ with $du/dt > 0$. If the period is approximated at the period $T(I_n)$ of the limit-cycle oscillation for the constant I shown in Fig. 10(a), the increase of I during the period is evaluated at $\epsilon'T(I_n)/T_p$, and therefore Eq. (20) is derived. The stationary state $I_{n+1} = I_n = I_s$ is obtained when $T(I_s)$ is equal to T_p and therefore $\epsilon'T(I_s)/T_p - \epsilon' = 0$ in Eq. (20). If the stationary solution is a stable solution in the mapping Eq. (20), the feedback control succeeds, and the target frequency $1/T_p$ is obtained by the time evolution of Eq. (19). The substitution of $T(I_n)$ in Fig. 10(a) into Eq. (20) yields a plot of I_n and I_{n+1} . Figure 13(b) shows the mapping Eq. (20) using $T(I)$ in Fig. 10(a) at $b = 1$. It is close to the plot in Fig. 13(a) obtained by the direct numerical simulation. The period-doubling bifurcation occurs when $dI_{n+1}/dI_n = -1$ in Eq. (20). The critical point of the period-doubling bifurcation

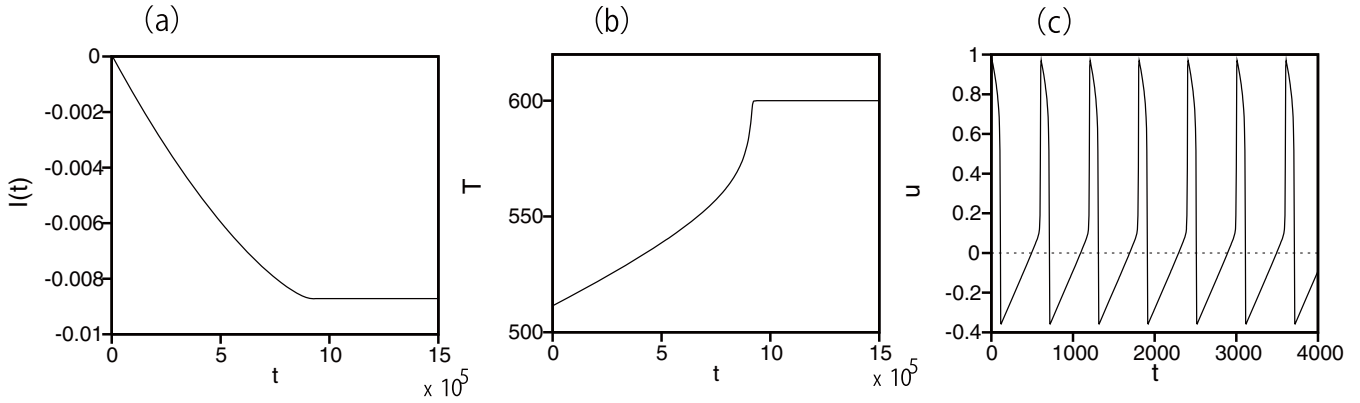


FIG. 11. (a) Time evolution of I at $T_p = 600$, $\epsilon' = 0.00005$, and $b = 1$. (b) Time evolution of the period of each pulsation at $T_p = 600$, $\epsilon' = 0.00005$, and $b = 1$. (c) Time evolution of u for $T_p = 600$ after the feedback control.

is estimated as

$$\left| \frac{dT}{dI} \right| = 2 \frac{T_p}{\epsilon'}, \quad (21)$$

because $dT/dI < 0$ in Fig. 10(a). For $\epsilon' = 0.00005$, the critical value is estimated as $T_{pc} = 609.3$ using Eq. (21). For the smaller parameter of $\epsilon' = 0.00001$, the critical value is $T_{pc} = 617.0$. These results are consistent with the direct numerical simulation shown in Figs. 12(a) and 12(b), that is, the approximation using Eq. (21) for the critical value is rather good.

In brains, there are various types of neurons. Some neurons exhibit bursting, where the spiking and nonspiking periods alternate. That is, the neuron exhibits spikes several times and then stops the spiking during the succeeding interval period. There are various model equations for the burst phenomena such as the Hindmarsh-Rose model and Plant-Kim model [16,17]. In general, a long timescale dynamics other than the spiking dynamics is involved in the burst firing. For example, a low-threshold Ca^{2+} current with a long timescale is involved in the burst firing in some neural systems [18]. We construct a

simple model based on the FitzHugh-Nagumo model as

$$\begin{aligned} \frac{du}{dt} &= u(u+a)(1-u) - v + I_e - I_i + I_0, \\ \frac{dv}{dt} &= \epsilon'(u-v), \\ \frac{dI_e}{dt} &= \epsilon'(A\delta(u-u_0)\theta(du/dt) - I_e), \\ \frac{dI_i}{dt} &= \epsilon''(B\delta(u-u_0)\theta(du/dt) - I_i), \end{aligned} \quad (22)$$

where I_e and I_i are interpreted as excitatory and inhibitory currents of long timescales induced by the spiking, and ϵ' and ϵ'' are decay constants respectively for I_e and I_i . When the FitzHugh-Nagumo oscillator is excited and u goes over u_0 , I_e and I_i jump by $A\epsilon'$ and $B\epsilon''$. Then, I_e and I_i decay with damping rate ϵ' and ϵ'' . I_0 is a constant input. When the FitzHugh-Nagumo oscillator is excited, the excited state continues for a while by the excitatory input I_e and then the suppressed state continues for a long time by the inhibitory input I_i , since ϵ'' is set to be smaller than ϵ' . Figure 14(a) shows the time evolution of u at $A = 1.5$, $B = 3$, $\epsilon' = 0.001$, $\epsilon'' = 0.0001$, and $I_0 = -0.008$. The spiking repeats six times,

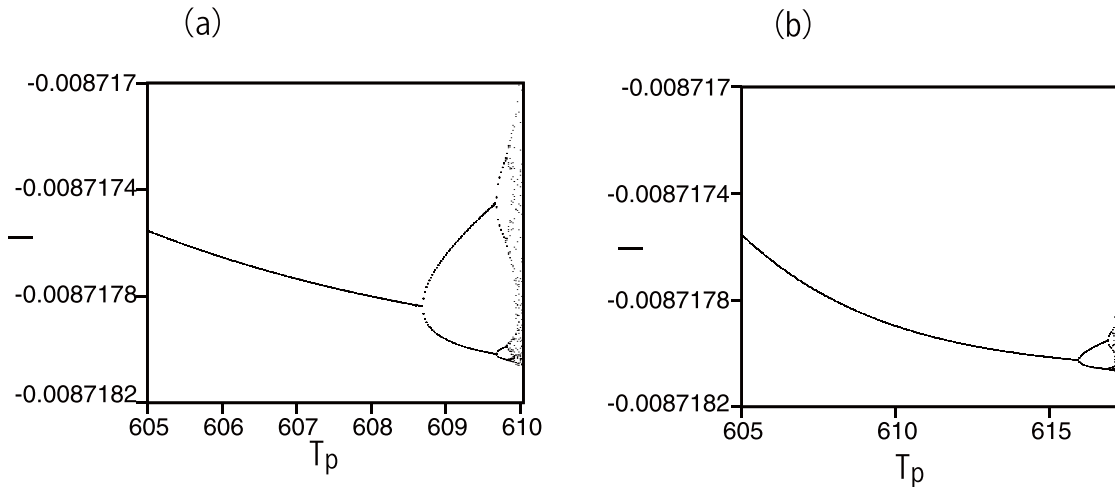


FIG. 12. (a) Relationship between T_p and the period after the feedback control at $b = 1$ for $\epsilon' = 0.00005$. (b) Relationship between T_p and the period after the feedback control at $b = 1$ for $\epsilon' = 0.00001$.

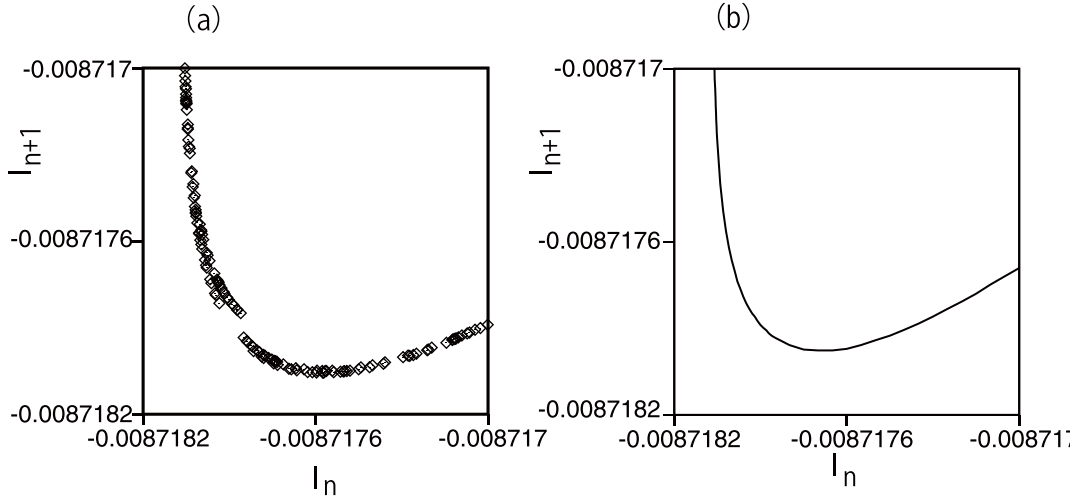


FIG. 13. (a) Relationship between I_n and I_{n+1} at $T_p = 609.93$ for $\epsilon' = 0.0005$. (b) Relationship between I_n and I_{n+1} by Eq. (20) at $T_p = 609.93$ for $\epsilon' = 0.0005$.

and then the nonspiking state appears. The total period is $T = 16268.2$ at the parameter values. We propose a feedback control method similar to Eq. (19) to generate the burst phenomenon with a target period T_p as

$$\begin{aligned} \frac{du}{dt} &= u(u+a)(1-u) - v + I_e - I_i + I_n, \\ \frac{dv}{dt} &= \epsilon(u-v), \\ \frac{dI_e}{dt} &= \epsilon'[A\delta(u-u_0)\theta(du/dt) - I_e], \\ \frac{dI_i}{dt} &= \epsilon''[B\delta(u-u_0)\theta(du/dt) - I_i], \\ \frac{dI}{dt} &= \epsilon''' \left(\frac{1}{T_p} - \delta(u-u_0)\theta(du/dt)\theta(T_n - t_m - T_0) \right). \end{aligned} \quad (23)$$

The input I_n takes a constant value $I(T_n)$ between $T_n \leq t < T_{n+1}$, where T_n is the time just before the passage through $u = u_0$ with $du/dt > 0$ satisfying $T_n - t_m > T_0$. Here, t_m is the last time when u passes u_0 with du/dt . That is, T_n is the passage time of $u = u_0$ after a long interval of the nonspiking

state. Figure 14(b) shows the time evolution of I_n starting from $I(t) = 0$ at $t = 0$ for $T_p = 16268.2$, $\epsilon''' = 0.0001$ and T_0 is set to 3000 to generate the burst phenomenon with a nonspiking interval larger than 3000. The other parameters are set to be $A = 1.5$, $B = 3$, $\epsilon' = 0.001$, and $\epsilon'' = 0.0001$. I_n approaches -0.008 finally. Figure 14(c) shows the time evolution of u by Eq. (23). The bursting time sequence with period T_p is reproduced.

Thus, we have shown that the spiking and bursting time sequences with target periods can be generated with feedback control.

V. SUMMARY

In this paper, We have considered a few control methods for the spiking phenomenon from the viewpoint of nonlinear dynamics.

First, we have studied the suppression of repetitive spiking by the periodic forcing in the FitzHugh-Nagumo model. The periodic solution of small amplitude is stabilized by the fast periodic modulation. It is analogous to the stabilized inverted pendulum by a periodic modulation. We have found

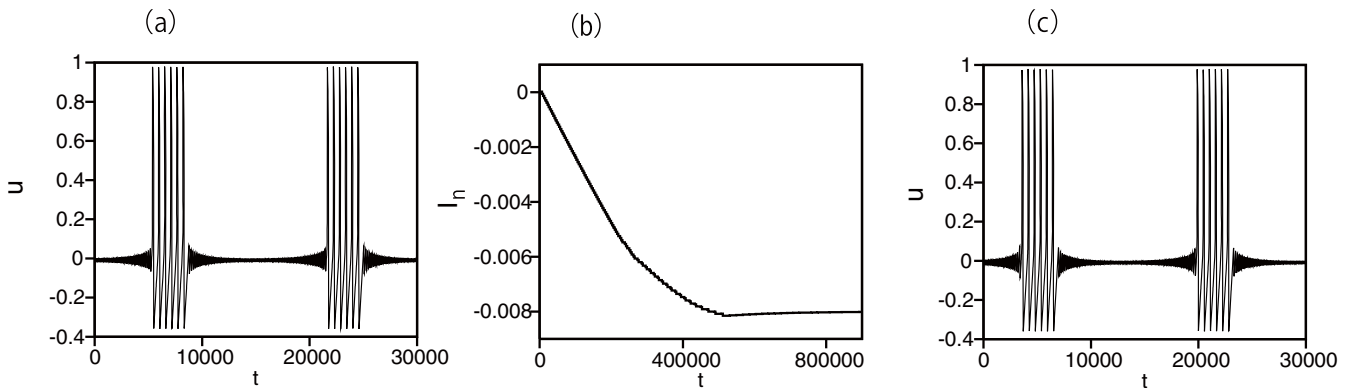


FIG. 14. (a) Time evolution of u by Eq. (22) at $A = 1.5$, $B = 3$, $\epsilon' = 0.001$, $\epsilon'' = 0.0001$, and $I_0 = -0.008$. (b) Time evolution of I_n by Eq. (23) starting from $I(t) = 0$ at $t = 0$ for $T_p = 16268.2$ and $T_0 = 3000$. (c) Time evolution of u by Eq. (23).

two boundary lines for the suppressed state in the FitzHugh-Nagumo model. We have found that there is a minimum value for the amplitude F of the periodic forcing to achieve the suppression in the FitzHugh-Nagumo model and the Hodgkin-Huxley model. The existence of the threshold of the amplitude for the spike suppression is the main result of this paper.

Next, we have studied globally and randomly coupled FitzHugh-Nagumo oscillators to study the suppression of repetitive spiking in the neural network. We have found that the periodic forcing makes the single FitzHugh-Nagumo equation chaotic, and the total sum of spiking becomes small owing to the chaos-induced desynchronization. Although these dynamical behaviors are interesting, both the single FitzHugh-Nagumo model and coupled FitzHugh-Nagumo os-

cillators are too simple as model systems to apply directly to actual neural networks in the basal ganglia, which is closely related to Parkinson's disease. We would like to apply our methods to more biologically relevant model equations in the future.

Finally, we have proposed a feedback method of the input to control the spiking frequency. Since the output signal of a neuron is often represented in the spiking frequency, it is important to control the spiking frequency. The feedback control method could be analyzed with the mapping of the input I_n . Furthermore, we have assumed long-timescale currents I_e and I_i induced by the spiking of the FitzHugh-Nagumo oscillator to generate the burst phenomenon and applied the feedback method to control the total period of bursting.

-
- [1] A. L. Hodgkin and A. F. Huxley, *J. Physiol.* **117**, 500 (1952).
 - [2] R. FitzHugh, *Biophys. J.* **1**, 445 (1961).
 - [3] J. Nagumo, S. Arimoto, and S. Yoshizawa, *Proc. IRE.* **50**, 2061 (1962).
 - [4] A. V. Holden, *Biol. Cybern.* **21**, 1 (1976).
 - [5] S. Rajasekar and M. Lakshmanan, *Physica D* **32**, 146 (1988).
 - [6] E. Ott, C. Grebogi, and J. A. York, *Phys. Rev. Lett.* **64**, 1196 (1990).
 - [7] K. Pyragas, *Phys. Lett. A* **170**, 421 (1992).
 - [8] P. A. Tass, *Phys. Rev. E* **66**, 036226 (2002).
 - [9] E. Adomaitienė, S. Bumelienė, and A. Tamaševičius, *Phys. Lett. A* **431**, 127989 (2022).
 - [10] A. L. Benabid, A. Benazzous, and P. Pollak, *Mov. Disord.* **17**, S73 (2002).
 - [11] K. Pyragas, V. Novicenko, and P. A. Tass, *Biol. Cybern.* **107**, 669 (2013); K. Pyragas and P. A. Tass, *Lith. J. Phys.* **56**, 223 (2016).
 - [12] H. Fujisaka and T. Yamada, *Prog. Theor. Phys.* **69**, 1 (1983).
 - [13] L. M. Pecora and T. L. Carroll, *Phys. Rev. Lett.* **64**, 821 (1990).
 - [14] H. Sakaguchi, *Phys. Rev. E* **61**, 7212 (2000).
 - [15] M. Gerster, R. Berner, J. Sawicki, A. Zakharova, A. Škoch, J. Hlinka, K. Lehnertz, and E. Schoöll, *Chaos* **30**, 123130 (2020).
 - [16] J. L. Hindmarsh and R. M. Rose, *Proc. R. Soc. Lond. B* **221**, 87 (1984).
 - [17] R. E. Plant and M. Kim, *Biophys. J.* **16**, 227 (1976).
 - [18] J. A. Beatty, M. A. Sullivan, H. Morikawa, and C. J. Wilson, *J. Neurophysiol.* **108**, 771 (2012).